

Low-energy electron diffraction study of potassium adsorbed on Ni(111)

Sumant Chandavarkar and Renee D. Diehl

Department of Physics, University of Liverpool, Liverpool L69 3BX, United Kingdom

(Received 7 April 1988)

Low-energy electron diffraction (LEED) data are presented for submonolayer coverages of potassium on Ni(111) at $70\text{ K} < T < 450\text{ K}$. Several incommensurate phases are observed which differ in their degree of order. At low coverage, rings are observed in the LEED pattern which are attributed to an amorphous solid or a fluid phase. At coverages between 0.14 and 0.22 monolayer, a hexagonal solid structure is observed which disorders into a correlated fluidlike phase before disordering completely. At a coverage of 0.25, the overlayer has a commensurate 2×2 structure, which is more stable than the incommensurate structures. The dominant interaction at all coverages appears to be the repulsive dipole interaction. Density modulations in the incommensurate layer, if they exist, are very weak. A phase diagram is presented.

INTRODUCTION

Much effort in surface physics has been dedicated to the understanding of the ordered phases of adsorbates. Recently there has been a growing interest in alkali-metal adsorption because much of the physics of submonolayers of alkali metals is observed to be very similar to that of rare-gas overlayers, which were originally studied for their simplicity. There is already a large body of theoretical work dealing with the phases produced in simple adsorption systems. Alkali metals are observed to be very highly mobile on smooth metal surfaces and to form equilibrium phases which can be either commensurate or incommensurate with the substrate. When alkali metals adsorb on metal surfaces, the charge transfer between the adsorbate atoms and the substrate (or, alternatively, the polarization of the adatom) results in the formation of a static dipole moment at each adatom, oriented perpendicularly to the surface. At low coverages, the repulsive dipole-dipole interactions are thought to dominate the equilibrium structures with the indirect interactions producing perturbations which affect the details of the structure. While there have been many studies of alkali-metal adsorption on the refractory metals where commensurate structures seem to prevail, many recent experiments have turned to alkali-metal adsorption on nonrefractory transition metals, where the substrate periodicity has a less obvious role in the determination of equilibrium surface structures. The reason for this difference is not well understood, although both theoretical and experimental studies indicate that the potential modulations along a direction parallel to the surface may be larger for alkali metals on refractory metal substrates. In this paper we present low-energy electron diffraction (LEED) data for potassium adsorption on a Ni(111) surface. The low-density submonolayer LEED patterns are similar to those previously observed for Na/Ru(001),¹ Na/Ni(111),² and Cs/Cu(111).³ We find that over most of the coverage range, the structure is hexagonal incommensurate having at most very weak density modulations.

EXPERIMENT

The experiments were carried out in a turbo-pumped stainless-steel ultrahigh vacuum chamber which has a base pressure of 4×10^{-11} mbar. The chamber was equipped with a cylindrical mirror analyzer (CMA) Auger system which was mounted on a bellows so that it could be moved out of the way when it was not being used. The homemade LEED optics is similar in design to that of Chinn and Fain⁴ and consists of a Cliftronic CE406W electron gun, with a 0.002 in. aperture, a 3-mm-i.d. stainless-steel drift tube, a single channel plate to amplify the diffracted electrons, and a phosphor screen. The major difference between Fain's LEED optics and ours is that instead of four hemispherical grids used to suppress inelastic electrons, this system has one flat grid kept at ground potential; the front of the channel plate is used to suppress inelastic electrons. This has the advantage of no distortion in the diffraction pattern due to grid wires, but the disadvantage that inelastic electrons are not uniformly suppressed across the screen. With a uniform suppressing voltage across the front of the channel plate, the electrons at large diffraction angles which have a smaller component of velocity perpendicular to the plate are suppressed more strongly than those nearer the center of the screen. For a case where the electrons at the edge of the screen are just cut off, i.e., where the perpendicular component of their velocity is equal to $(2E/m)^{1/2}$ (E is the primary beam energy and m is the electron mass), the electrons hitting the center of the screen will be suppressed if their energy is less than about 75% of the primary beam energy. Thus, the inelastic cutoff is 25% higher at the edge of the screen than at the center. Since we do not make quantitative measurements of the relative intensities of spots here, and since we can choose the suppressor voltage to optimize the spot we are measuring, we feel that our results are not affected very much by the nonuniform suppression. Our spot profiles are measured across at most 5% of the screen radius, thus suppression will not vary appreciably across the spot. The LEED pattern was viewed and photographed

by use of a mirror positioned at 45° to the phosphor screen and to a viewport. 400 ASA black-and-white or color film was used to record LEED patterns.

The $7 \times 4 \times 2\text{-mm}^3$ Ni(111) crystal was cut from a high-purity single-crystal rod using a spark-erosion cutter and then oriented using Laue x-ray diffraction. A spark-planing technique was used to make fine adjustments to the surface orientation, and the final surface was measured to be (111), accurate to within $<0.5^\circ$. The (111) surface was prepared by polishing with a diamond polishing compound down to $1\text{-}\mu\text{m}$ particle size. Two 0.25-mm holes were spark eroded into two opposite edges of the crystal. After checking the orientation again with Laue diffraction, the crystal was mounted on the UHV sample holder by means of four 0.25-mm Ta wires which fit into the holes in the crystal. These wires were spot welded to two Ta plates on either side of the crystal. The Ta plates were electrically isolated from the rest of the manipulator-sample-holder by thin alumina slabs. The crystal was thus rigidly suspended between two Ta plates which were electrically isolated from the rest of the system. The crystal could be heated to 1000 K by passing a current of 12 A through it. This resulted in a resistive heating of the Ta support wires and thermal conductive heating of the Ni crystal. An optical pyrometer was used to check the uniformity of heating across the Ni crystal, and it was found to be uniform to within 6° at 1000 K. The sample holder itself was mounted on the cold finger of a Heli-tran refrigerator. The crystal could be cooled to 120 K using liquid nitrogen, or to 50 K using liquid helium. The temperature of the crystal was measured using a Chromel-Alumel thermocouple spot welded to the back of the crystal and an electronic reference temperature.

The crystal was cleaned by cycles of bombardment with 0.5 or 1.0-keV Ar^+ ions for 45 min and then heating to 1000 K. The cleanliness of the crystal was monitored using Auger-electron spectroscopy (AES). The primary contaminants initially were carbon and sulfur. After cleaning for about two weeks, no contaminants could be observed by AES immediately after bombardment and annealing to 1000 K. After this, subsequent Ar^+ bombardment was for shorter times with a defocused ion beam. We found that a more gentle bombardment produces a more perfect surface as judged from the LEED pattern of both the clean surface and that with adsorbed potassium. The detrimental effects of ion bombardment have also been observed in H adsorption experiments on Ni(111).⁵ The crystal remained clean to within AES detectability for several hours after cleaning if no alkali metal was evaporated onto it.

Potassium was evaporated onto the Ni crystal using a SAES Getters source. The source was degassed at a current of 3 A for at least three days before experiments were carried out. The system pressure was not allowed to rise higher than 5×10^{-9} mbar during the outgassing period. For most of these experiments, the source was surrounded by a liquid-nitrogen cold trap which was used to trap the CO emitted by the source. CO was the largest measurable impurity from the source. When the source was carefully degassed and the liquid-nitrogen trap operating, the pressure of the system did not rise above

the base pressure during evaporation. If the liquid-nitrogen trap was not in use, the pressure rise was not more than 3×10^{-10} mbar, but there was always some CO adsorption onto the surface which could be detected by AES. The potassium source was located approximately 10 cm from the crystal during K deposition, and was usually operated at 6.5 A. At this current, a coverage of 0.25 monolayers was achieved after approximately 110 s, depending on the individual K source. A shutter was used in front of the source to facilitate accurate timing. The coverage was determined in these experiments by measuring the dose of K required to form a 2×2 pattern, which will be described in the following section. This coverage was defined to be 0.25 monolayers, and other coverages were calculated assuming that the dosing rate was reproducible. Auger measurements indicated that there was a constant sticking coefficient for submonolayer coverages. This method of determining the coverage gave reproducible results from experiment to experiment and also for different K sources. In this sense, this method was preferable to using Auger-electron spectroscopy to calibrate the sources, since each new source would require recalibration using AES. The major source of uncertainty in our LEED method arises from the possibility of filling defect sites during the initial evaporation of K onto the crystal. This apparently was a small effect, since our coverages calculated from the LEED method described above agreed well with inferred lattice constants over a wide coverage range, which will be described in the next section.

The analysis of the LEED patterns was carried out by digitizing the photographic negatives using a microdensitometer at Daresbury Laboratory. A square area the size of the LEED screen was digitized to a resolution of $25\ \mu\text{m}$ and then analyzed using standard programs existing at Daresbury. The film density correction to the densitometer intensity was made analytically. Spot profiles and distances between spots could be easily extracted from the digital data. A flat-plate correction, to account for the imaging of the LEED pattern onto a flat screen, was made after the data were digitized.

RESULTS

The LEED pattern from the clean Ni(111) surface has a low background intensity and sharp spots with a marked threefold symmetry which varies as a function of energy. Threefold symmetry is expected from the (111) surfaces of fcc metals since the surface layer is threefold symmetric with respect to the second layer, and this symmetry is maintained across steps. As the potassium is evaporated onto the Ni surface, the first change in the LEED pattern is the appearance of rings around each of the Ni spots, including the specular beam. These rings are first detectable at approximately 0.05 monolayers coverage and as the coverage is increased, the diameter and intensity of the rings increases. [A coverage of one monolayer is defined as having the same number of atoms as in a perfect Ni(111) surface layer. One physical monolayer, which will be discussed later, consists of one close-packed layer of adsorbate atoms, and occurs at a cover-

age of approximately 0.31 for K/Ni(111).] At 0.12 monolayers, the rings begin to coalesce into spots which are rotationally aligned along the Ni(111) sixfold symmetry directions. Since the spots have the same magnitude of momentum transfer as the rings, it is difficult to judge the width of the spots when they first appear. However, as the coverage is increased further, the intensity of the spots increases as the intensity of the rings decreases while both spots and rings continue to move to larger momentum transfers with respect to the centers of the rings. At 0.18 monolayers, the rings are no longer visible, and the LEED pattern could be described as consisting of groups of split spots, each group centered on a 2×2 reciprocal-lattice position. As the coverage is further increased, the splitting of these spots gradually decreases until there is no measurable splitting and the pattern is consistent with a 2×2 superlattice. This is the structure which is defined as having a coverage of exactly 0.25 monolayers. Above this coverage, the spots again split with the splitting increasing as the coverage increases. LEED patterns corresponding to this progression are shown in Fig. 1 for adsorption at 120 K.

LEED patterns for adsorption of potassium at 70 K showed no essential difference from those for adsorption at 120 K. At coverages between 0.18 and 0.22 monolayers, where the patterns consisted primarily of spots rather than rings, heating the crystal to about 185 K caused the spots to become broader in both the radial and azimuthal directions. This broadening was reversible in temperature and appears to be an intrinsic property of the layer. These diffuse spots then disappeared at about

350 K. Between the coverages of 0.22 and 0.28 monolayers heating the crystal to about 225 K caused the spots to become sharper in both the radial and azimuthal directions. This spot sharpening at 225 K was irreversible and it suggests that although the structure can readjust its density quickly after deposition of potassium (within several seconds), it may not be in complete equilibrium, especially with respect to its rotational alignment. It seems likely that at the lower temperatures, the layer is unable to "anneal" into large crystallites. The equilibrium structures at coverages above 0.18 monolayers and below 180 K seem to be well aligned along the Ni(111) symmetry directions, although for coverages above 0.25 monolayers, there usually was a small amount of rotational broadening even after the layer was heated to the disordering temperature and allowed to cool. The data obtained by evaporating the K on the surface at 300 K agrees well with that obtained when the K was evaporated onto the surface at 120 K and the surface was subsequently heated to 300 K.

The LEED patterns were very sensitive to impurities and possibly to the defect density of the surface. The effect of a small amount of oxygen or carbon monoxide contamination was to produce sharper spots in the LEED patterns. Presumably these impurities have the effect of stabilizing or pinning the K structure. In experiments where there were no detectable impurities, there were variations from experiment to experiment in the width of the overlayer LEED spots. This variation is probably due to the effects of surface defects on the equilibration of the overlayer. At low temperatures, while the mean den-

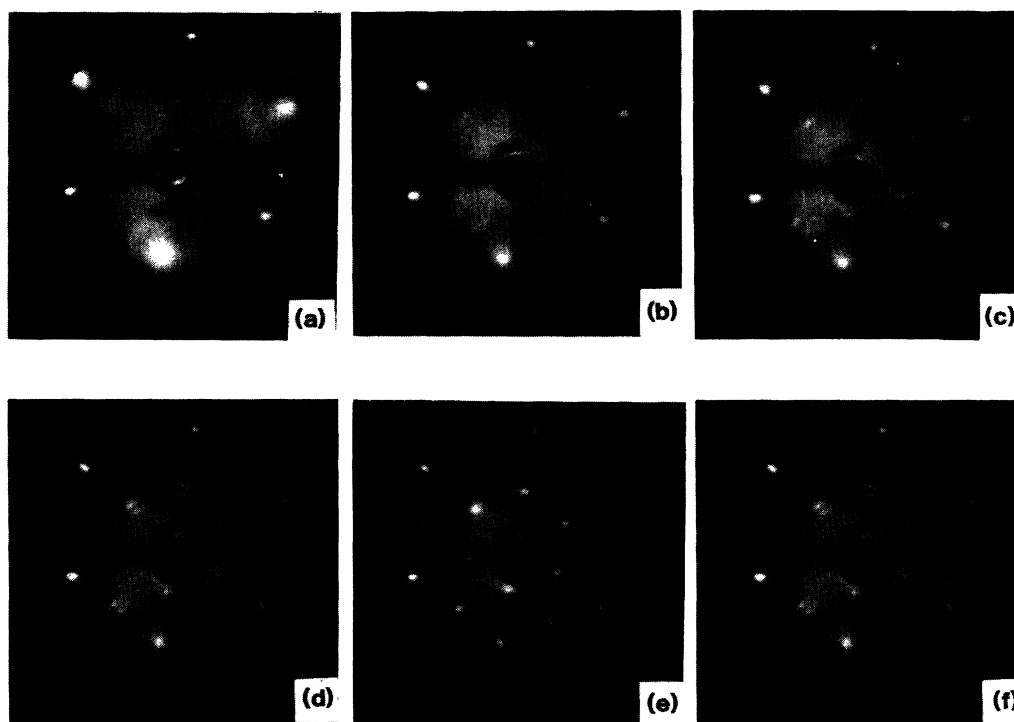


FIG. 1. LEED patterns for adsorption of potassium at 120 K. Coverages are (a) 0.11, (b) 0.14, (c) 0.18, (d) 0.20, (e) 0.25 (f) 0.29 monolayers. All photographs were taken at primary electron beam energy $E = 192$ eV, except for (a), which was at 181 eV. The specular beam would be just above the center of the pattern if it were visible, and the six outermost bright spots are from the Ni(111) surface. Note that the threefold symmetries of the substrate and multiple diffraction rings are apparent in (a).

sity appeared to equilibrate very quickly after deposition, there were often local regions having different densities at different places on the crystal. This effect could be maximized by evaporating K only on part of the crystal. Even in this case, however, there were large areas of the crystal on which the K density was apparently uniform. We think that the effect of defects, which are probably mostly surface steps, is to hinder the diffusion of potassium from terrace to terrace, although in regions which have few steps, the K diffuses rapidly. This slow migration across steps may be due to K adsorbed more strongly at step sites, effectively slowing the passage of other K atoms. Heating the crystal caused the potassium density to become more uniform across the crystal, although there were sometimes still local regions of higher or lower density, especially near the edges of the crystal where the defect density may be higher. To see the effect of surface defects, we purposely produced surfaces having a higher defect density by ion bombarding for 5 min before adsorbing potassium. In those experiments, while there were definite gradients on the surface, there was no appreciable difference in the LEED patterns observed from those observed on more perfect surfaces, except that the patterns were more diffuse. In the experiments presented here, we minimized the density gradients by carefully annealing the crystal before depositing K, adsorbing K as uniformly as possible, and by always making measurements on the same area of the crystal in each experiment.

DISCUSSION

When viewing the diffraction rings at low coverage as a function of energy, a threefold symmetry in the rings around the first-order Ni spots was apparent, i.e., the rings around three of the spots had a different intensity versus energy dependence than that of the other three spots. This energy dependence tracked with the energy dependence of the first-order Ni spots. Thus, we attribute the rings around the nonspecular Ni beams to a double scattering by one first-order K-overlayer reciprocal-lattice vector plus one first-order Ni reciprocal-lattice vector. The rings must arise from a disordered overlayer, which could be either a fluid, an amorphous solid, or a polycrystalline solid. The coverage at which the rings give way to spots is the same at 70 and 120 K. The rings reversibly disappear at temperatures above 175 K, depending on the coverage, which indicates that a disordering transition occurs for the structure which produces the rings. The data are consistent with a solid phase, either polycrystalline or one in which the K atoms are randomly located on the surface, possibly in high-coordination sites, with a reasonably well-defined nearest-neighbor distance.^{1,2} In order to extract a mean nearest-neighbor distance L from our data, we used an approximation that the disordered structure was on average hexagonal and we determined a mean nearest-neighbor distance $L = (2/\sqrt{3})2\pi/\Delta S_{\text{parallel}}$, where $\Delta S_{\text{parallel}}$ is the momentum transfer of the peak of the ring intensity relative to the center of the ring. We measured the $\Delta S_{\text{parallel}}$ from our photographs relative to the momentum transfer of the first-order Ni spots, and assumed a Ni-Ni distance of 2.49 Å.⁶ The mean nearest-neighbor distance L thus ob-

tained is plotted in Fig. 2 as a function of coverage. It is consistent with the curve of L expected for a uniform contraction of a hexagonal layer. This is more easily seen in the graph of L^{-2} versus coverage. L^{-2} can be thought of as the mean area density of the layer, and the data follow the straight line expected for a perfect hexagonal layer up to 0.31 monolayers. Above this coverage, potassium begins to go into the second layer, although the mean density of the first layer continues to increase slowly. For the low-coverage "ring" phase, we might expect a slight difference between our L and the true nearest-neighbor distance, since the intensity distribution

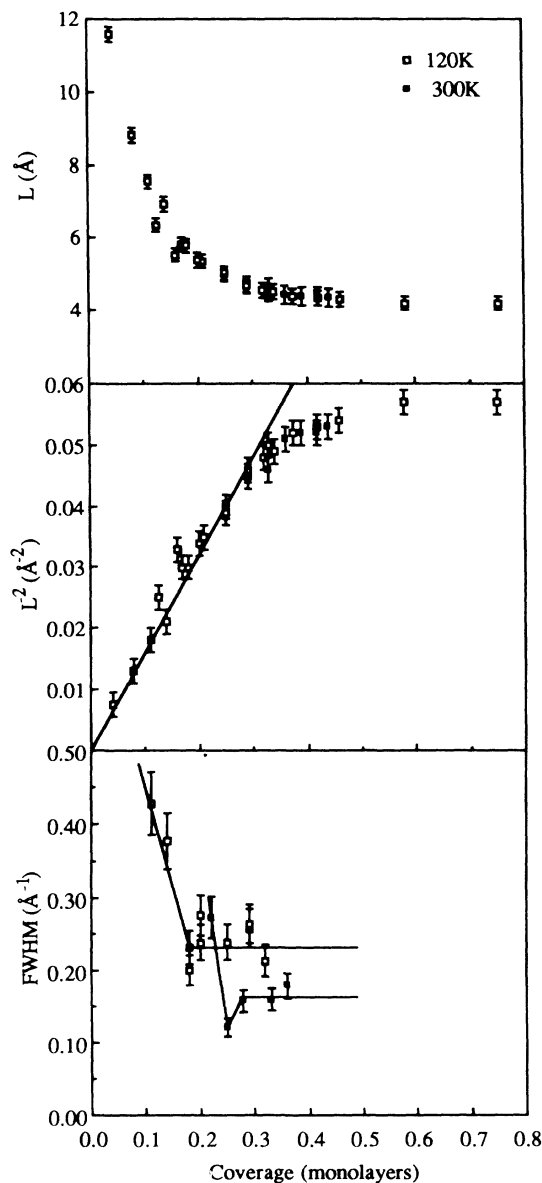


FIG. 2. Mean nearest-neighbor distance L , L^{-2} , and full width at half maximum (FWHM) of first-order potassium diffraction beams in the radial direction as a function of coverage. The data are from several experimental runs at 120 K and one at 300 K. The line shown in the graph of L^{-2} is that which would be expected for a uniform compression of a hexagonal overlayer.

rather than just the maximum in the intensity distribution should be transformed. However, due to the narrowness of the rings in the radial direction, this correction is probably within the precision of our measurements. A similar analysis was carried out on a different system of repulsive dipoles, that of Xe/Pd(100) (Ref. 7) for which rings were observed over a large coverage range. In that case, the curve of L versus coverage did not follow the curve expected for a hexagonal lattice at the lower coverages, possibly due to a "melting" of that structure. No such departure was seen for our data at either 120 or 300 K. This may be further evidence that the potassium ring phase is a solid phase rather than a fluid. The temperatures at which the rings disappear are indicated in the phase diagram in Fig. 3. This disappearance is attributed to a disordering of this phase and is reversible in temperature, although there appears to be some hysteresis.

The lack of rotational order and apparent incommensurability with the substrate at low coverage contrasts with the results on refractory metals, where very long-period, well-ordered commensurate structures are observed when the temperature is lowered enough to limit thermal mobility of the adsorbed atoms.⁸ This may be due to a difference in the lateral surface-potential modulation relative to other interadsorbate interactions. By lateral surface-potential modulation, we mean the variation of the potential energy of an adsorbed atom as it moves across the surface at a constant distance z from the surface. The lateral potential modulation will result from the hard-core repulsion of substrate atoms, the Friedel oscillations which result from the displacement of surface electrons, and the oscillatory substrate-mediated (indirect) interactions. At intermediate distances on low-index planes of transition metals, the indirect interactions are predicted to be the largest.⁹ These interactions are

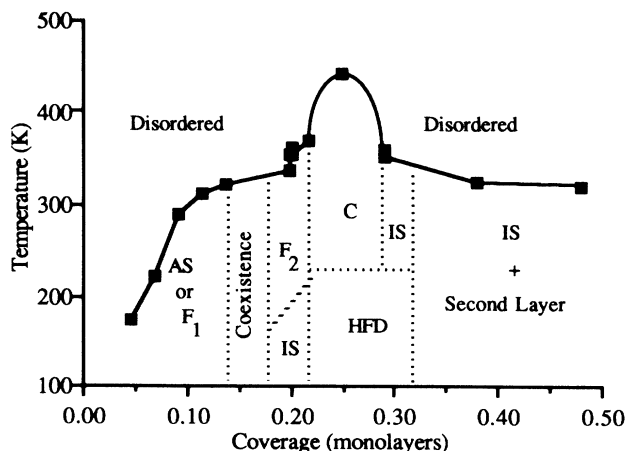


FIG. 3. Phase diagram for K/Ni(111). The data points were obtained by observation of the disappearance and appearance of diffraction rings or spots as a function of temperature. The dotted lines are inferred from the LEED data obtained in experimental runs at either constant temperature or constant coverage. The labeled phases are AS, amorphous solid; F_1 , low coverage fluid; F_2 , fluid; IS, incommensurate solid; C, 2×2 commensurate solid; FD, hexagonal with frozen-in disorder; IS, incommensurate solid. The width of the commensurate region shown is the upper limit on the true width.

known to play a role in the ordering of alkali metals on W and Mo surfaces, but the details of their effect are difficult to calculate because they are very sensitive to the details of the Fermi surface of the material.⁹ The experimental evidence for the presence of indirect interactions in the case of alkali metals on refractory metals is that different commensurate structures are observed on the very similar surfaces of W and Mo, which would be expected to be identical if there were no substrate-mediated interactions.¹⁰

Theoretical estimates¹¹ for the surface-potential modulation for alkali metals on Al jellium are very small, e.g., 2×10^{-3} meV for K on the (111) surface. Estimates for alkali metals on W(100) are in the range 0.01–0.1 eV.⁹ In order to estimate this interaction of K/Ni(111), we note that field emission microscopy (FEM) experiments on W(100) and Ni(111) (Ref. 12) show that the surface diffusion barrier, which is related to the lateral potential, is generally around a factor of 2–3 smaller for Ni than for W. Therefore, making a crude analogy between Ni(111) and W(100) we estimate the lateral potential modulation for K/Ni(111) to be not larger than about 0.05 eV in the density range of interest, and probably much smaller at the densities at which we observe the ring patterns. An additional coverage dependence of the relative size of this potential will probably arise due to the adsorption distance z increasing as a function of coverage due to depolarization as observed for Cs/Ag(111),¹³ but we could find no theoretical estimates of this effect. Our estimate for the lateral surface modulation should be compared with the interadsorbate dipole-dipole repulsion energy. Although work-function data are not available for K/Ni(111), it can be estimated from the trends observed by Gerlach and Rhodin² for sodium adsorbed on Ni(111), Ni(100), and Ni(110), and potassium and cesium adsorption on Ni(110). Using the Helmholtz equation relating dipole moment to work function,¹⁰ we estimate that the dipole moment per adatom for K/Ni(111) will vary from approximately 7 to 4 D over the range of coverage of 0–0.31 monolayers of K. From this dipole moment, the calculated dipole-dipole repulsion energy is of the order of 0.06 eV at a coverage of 0.06, and 0.32 eV at a coverage of 0.25, which is larger than our estimate of the lateral potential energy modulation. If these estimates are correct, the interatomic distances would be determined mainly by the repulsive interatomic adsorbate interactions, which are probably not sufficiently anisotropic at low coverage (large nearest-neighbor distances) to introduce azimuthal ordering.

At coverages between about 0.15 and 0.18 monolayers, there is an azimuthal intensity variation in the diffraction rings which might be interpreted as a coexistence of two K phases, one azimuthally orientated along the Ni $\langle 10 \rangle$ directions and one randomly oriented. However, both phases would apparently have the same density, and such a solid-solid coexistence seems unlikely. An alternative explanation is that this is a single phase which has regions of slightly different densities due to surface heterogeneity. This explanation could be correct if at some critical coverage, the depolarization of the potassium becomes significant enough that the balance of the lateral

interactions changes as a result of the dipole-dipole repulsion decreasing relative to other interactions. This does not, however, explain why the K lattice ultimately aligns itself along the Ni $\langle 10 \rangle$ direction in spite of the fact that it is apparently incommensurate. To investigate this, we look at the coverage range $0.18 < \Theta < 0.22$ monolayers where the rings are no longer detectable. In this coverage range, at temperatures below 185 K, the LEED pattern is consistent with an incommensurate hexagonal K overlayer. The overlayer spots are split, and at least some of the intensity in the outside spot of each split-spot pair is due to multiple diffraction. The evidence for this is that at electron beam energies at which there is a strong threefold symmetry in the scattering from the Ni substrate, the outside spots of the split pairs (see Fig. 1), which are in positions consistent with a double scattering from one Ni (10) beam and one K (10) beam [assuming now that the inside beams correspond to K (10) beams] also show a very strong threefold symmetry. There are also weak beams on either side of the 2×2 positions (i.e., rotated with respect to those described above) which arise from the double scattering from one Ni (10) beam and one K (11) beam. The substrate-induced threefold symmetry is visible in these spots as well, although these beams are not visible at the energies shown in Fig. 1. This type of spot splitting can also be a result of antiphase domains in the overlayer. Our kinematic calculations¹⁴ show that the effect of antiphase domains, where each domain has a 2×2 structure, would be to split (2×2) overlayer spots into two intense spots and two weak spots, the two intense ones having approximately equal intensities and located at the same positions as our more intense spot pairs and the weak ones located at the positions of our weak pairs. But since at some primary beam energies one spot of each pair disappears completely while the other spot is still visible, the major source of the split spots is likely to be multiple diffraction. In addition, we also observe higher-order diffraction spots from the incommensurate overlayer which would not be present if there were strong density modulations. The assertion that these spots are multiple diffraction rather than due to domain-wall splitting leads to the conclusion that this incommensurate overlayer has at most very weak density modulations, or alternatively, very wide domain walls, which further suggests that the dominant interaction at low coverages is the dipole-dipole repulsion between K atoms, and that the effect of the substrate lateral potential energy is very small.

Steps on the surface might play a very important part in the orientation of the K layer, even though we have tried to minimize surface defects. One estimate of the lateral potential energy modulation on a stepped surface was made for K atoms on Al jellium¹¹ to be approximately 0.09 eV, or about 45 times larger than the flat-surface modulation. A diffusion barrier was actually measured for K adsorption on polycrystalline Ni, which might be thought of as the ultimate stepped surface, to be 0.44 eV (Ref. 15) compared to about 0.1 eV for flat Ni(111), which was inferred from FEM measurements.¹² This might be large enough to influence the rotational alignment of the K layer by causing the K atoms to adsorb preferentially

in the high-coordination sites along the Ni steps, when the terrace widths are small enough compared to the mean K-K spacing, thus forcing the orientation of the rest of the layer on the terraces, where the lateral modulation is much smaller, to also rotationally order along the steps. We measured our crystal using Laue diffraction to be flat to within 0.5° of the (111) plane. This leads directly to an upper limit for the terrace width of approximately 300 Å. This in itself does not guarantee large stepless terraces; so we measured the nickel (00) spot width as a function of energy as a means of finding a lower limit for the terrace width. A preliminary analysis of this data indicates that the step density is lower than the ability of the LEED instrument to detect them, and we estimate a lower limit on average terrace width to be about 150 Å. Since we find that at low coverage the ring patterns we observe have momentum transfers which are compatible with the density calculated from the amount of K evaporated onto the surface, and there is no evidence for azimuthal intensity modulations, we are reasonably sure that the amount of K adsorbing preferentially at step sites at coverage below about 0.15 monolayers must be small. We attribute this to the large dipole-dipole repulsion of the K atoms, which overrides the potential energy to be gained by having the K atoms at step sites. However, as the mean K-K distance decreases, more step sites become available at distances near to those compatible with the dipole repulsion between K atoms, and thus a higher proportion of atoms will go to step sites as long as there is even a small amount of potential energy to be gained.

In the same coverage range, alkali metals on Ru(001) appear to have the same structures as those observed for K/Ni(111), while at higher surface densities, which are inaccessible to the K/Ni(111) system because of the relative sizes of the Ni lattice and the K atoms, rotated incommensurate structures are observed.^{1,16} The aligned structure at low coverage may in fact be the lowest free-energy configuration on a perfect surface. However, the low-density layer is likely to be less rigid due to the greater separation of atoms and therefore may not be able to support a rigid rotation such as that predicted by Novaco and McTague,¹⁷ and in that case it may be more susceptible to the influence of surface steps. Such effects of surface defects pinning overlayer orientations have been observed in other adsorption systems.^{18,19} It is worth noting that LEED experiments done for Na,² Cs, and Li (Ref. 20) on Ni(111) also only show rotational ordering along the Ni symmetry directions at these coverages.

At coverages between 0.18 and 0.22 monolayers, the LEED spots rather abruptly become more diffuse in both the radial and azimuthal directions when the crystal is heated to about 185 K. This change is reversible. A detailed analysis of this phase has not been made, but the phase appears to be an independent phase, possibly a well-correlated fluid which then disorders at 350 K. A similar phase was observed in the case of Cs/Cu(111) (Ref. 3) at approximately these coverages, and it is interpreted as the hexatic phase which would be expected in the melting of a 2D solid. A detailed analysis of the spot

profiles in the radial and azimuthal directions is required to determine whether this phase truly has a hexatic nature for K/Ni(111).

The patterns we observe at coverages near 0.25 monolayers are indicative of a commensurate 2×2 structure. If the layer were commensurate (i.e., locked in) at a coverage of 0.25 we would expect significantly sharper spots due to the longer-range order in a commensurate phase. The radial spot widths are shown in Fig. 2 for adsorption at 120 and 300 K. At 120 K there is no indication of the layer locking in to the substrate lattice. This is apparently due to the frozen-in disorder discussed earlier. At 300 K the spot width of 0.25 monolayers is significantly sharper than those of the 120- and 300-K incommensurate solids. The disordering temperatures shown on the phase diagram in Fig. 3 give further evidence that the 2×2 phase is locked in to the substrate lattice, since the disordering temperature for the 2×2 phase is higher than those of the higher- or lower-density incommensurate structures. It is possible that the incommensurate structures at coverages very near to the 2×2 coverage form long-period domain walls, but it is impossible to determine this from our data. At mean densities at least 10% away from this density, there is no evidence for domain walls.

At coverages above 0.25 monolayers the overlayer diffraction spots split again in a similar way to the lower-coverage split spots. This splitting is also attributed largely to multiple scattering, for the same reasons as in the low-density case. Above 0.25 monolayers, the hexagonal overlayer compresses uniformly, within the resolution of these measurements, until 0.31 monolayers and an average nearest-neighbor distance of about 4.6 Å. Beyond this coverage, the lattice constant continues to decrease somewhat, but more slowly due to K going into the second layer. The ultimate K-K spacing observed was 4.2 Å at coverages above about 0.5 monolayers. For reference, the close-pack spacing in bulk K is 4.54 Å at 78 K.⁶ This apparent reduction in the size of the atoms is typical in alkali-metal monolayers and is a result of the charge transfer on adsorption.² At coverages between about 0.28 and 0.31 monolayers, the incommensurate hexagonal layer does not disorder via an intermediate phase as in the case of the low-density incommensurate layer, but remains solid until its disordering temperature of about 340 K. Experiments to look for an ordered bilayer were carried out, but no new structures were observed. Therefore the second-layer structure is either disordered, has essentially the same structure as the first layer, or forms 3D crystallites on top of the first layer. The polarization of the second-layer atoms must be much smaller than for the first layer, possibly leading to net attractive interactions between adatoms and the formation of 3D crystallites. However, it is possible to grow oriented bcc alkali-metal crystals on certain metal surfaces, and therefore an ordered second layer is not out of the question.²¹ The disordering temperature for the overlayer at

high coverage is about 320 K. The bulk melting temperature for potassium is 337 K.

CONCLUSION

Unlike alkali-metal adsorption on the refractory metals, potassium adsorbed on Ni(111) does not form long-period commensurate structures even at low temperatures. The structures observed for potassium adsorption appear to be incommensurate over the whole range of coverage from zero to above one physical monolayer, except at a coverage near 0.25, where a commensurate 2×2 structure is observed. The interactions in the overlayer seem to be dominated by the repulsive dipole interactions, with the lateral interactions due to the substrate playing only a minor role in the equilibrium structures. The apparent lack of complete mobility of the potassium on the surface at low temperatures may also hinder the formation of commensurate phases. We cannot, however, rule out the possibility of higher-order commensurate structures having closely spaced densities such as those discussed by Doering²² in the orientationally ordered incommensurate phases. Doering has suggested the possibility that the rotational smearing observed in these phases might be a result of a competition between two branches of higher-order commensurate structures along different trajectories in lattice-spacing-epitaxial rotation space.^{22,23} It may be very difficult to distinguish such a mixture from an incommensurate phase even with very-high-resolution diffraction due to the distribution of domain sizes. It is interesting to note that incommensurate phases which are thought to be floating solid phases on a centered rectangular substrate were observed in Monte Carlo calculations where only the chemisorption bond and the dipole energies were included in the Hamiltonian.²⁴ In those calculations, many long-period structures were also observed at low coverage. It would be interesting to see the results of such calculations for a triangular substrate which has a four- or eight-sublattice-site array. The possibility that this type of incommensurate layer may provide realizations of the two-stage melting predicted for 2D solids²⁵ has already been suggested by Fan and Ignatiev.³ Further experiments on the melting of these layers should provide more insight into the characteristics of incommensurate layers and 2D solids.

ACKNOWLEDGMENTS

We gratefully acknowledge useful conversations with Sam Fain, Stephen Holloway, Jacques Jupille, Dale Doering, and Lyle Roelofs. We would also like to thank John Murray for his expert technical assistance. The experiments were carried out on an apparatus provided by United Kingdom Science and Engineering Research Council (SERC) Grant No. GR-D-09446 and data analysis was carried out with the support of SERC Daresbury Laboratory. One of us (S. C.), was supported by Liverpool University and by the Overseas Research Student Program.

- ¹D. L. Doering and S. Semancik, *Surf. Sci.* **129**, 177 (1983).
- ²R. L. Gerlach and T. N. Rhodin, *Surf. Sci.* **19**, 403 (1970); **17**, 32 (1969).
- ³W. C. Fan and A. Ignatiev, *J. Vac. Sci. Technol. A* **6**, 735 (1988).
- ⁴M. D. Chinn and S. C. Fain, *J. Vac. Sci. Technol.* **14**, 314 (1977).
- ⁵K. D. Rendulic, A. Winkler, and H. P. Steinrück, *Surf. Sci.* **185**, 469 (1987).
- ⁶R. W. G. Wyckoff, *Crystal Structures*, 2nd ed. (Wiley, New York, 1963), Vol. 1.
- ⁷E. R. Moog and M. B. Webb, *Surf. Sci.* **148**, 338 (1984).
- ⁸A. G. Naumovets, *Sov. Sci. Rev. A Phys.* **5**, 443 (1984).
- ⁹O. M. Braun, *Fiz. Tverd. Tela (Leningrad)* **23**, 2779 (1981) *Phys.—Solid State* **23**, 1626 (1981)].
- ¹⁰E. Bauer, in *Chemical Physics of Solid Surfaces and Heterogeneous Catalysis*, edited by D. A. King and D. P. Woodruff (Elsevier, Amsterdam, 1982), Vol. IIIa, and references therein.
- ¹¹L. M. Kahn and S. C. Ying, *Surf. Sci.* **59**, 333 (1976).
- ¹²R. Wortman, R. Gomer, and R. Lundy, *J. Chem. Phys.* **27**, 1099 (1957).
- ¹³G. M. Lamble, D. J. Holmes, D. A. King, and D. Norman, *J. Phys. (Paris) Colloq.* **46**, C8-509 (1986).
- ¹⁴P. Rowlands and R. D. Diehl (unpublished).
- ¹⁵M. Blaszczyzyn, *Surf. Sci.* **151**, 351 (1985).
- ¹⁶D. L. Doering and S. Semancik, *Phys. Rev. Lett.* **53**, 66 (1984); *Surf. Sci. Lett.* **175**, L730 (1986).
- ¹⁷A. D. Novaco and J. P. McTague, *Phys. Rev. Lett.* **38**, 1286 (1977).
- ¹⁸M. F. Toney and S. C. Fain, *Phys. Rev. B* **30**, 1115 (1984).
- ¹⁹K. Kern, P. Zeppenfeld, R. David, R. L. Palmer, and G. Comsa, *Phys. Rev. Lett.* **57**, 3187 (1986).
- ²⁰J. Jupille (private communication).
- ²¹I. R. Collins (private communication).
- ²²D. L. Doering, *J. Vac. Sci. Technol. A* **3**, 809 (1985).
- ²³D. L. Doering (private communication).
- ²⁴L. D. Roelofs and D. L. Kriebel, *J. Phys. C* **20**, 2937 (1987).
- ²⁵J. M. Kosterlitz and D. J. Thouless, *J. Phys. C* **6**, 1181 (1972); B. I. Halperin and D. R. Nelson, *Phys. Rev. Lett.* **41**, 121 (1978); A. P. Young, *Phys. Rev. B* **19**, 1855 (1979).

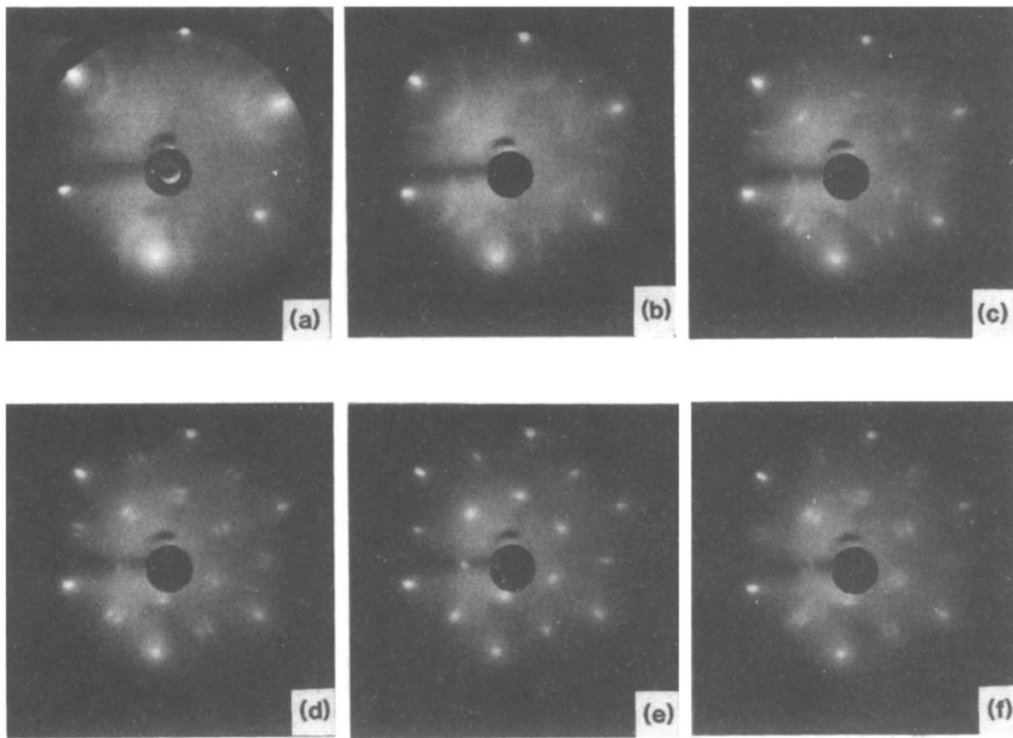


FIG. 1. LEED patterns for adsorption of potassium at 120 K. Coverages are (a) 0.11, (b) 0.14, (c) 0.18, (d) 0.20, (e) 0.25 (f) 0.29 monolayers. All photographs were taken at primary electron beam energy $E = 192$ eV, except for (a), which was at 181 eV. The specular beam would be just above the center of the pattern if it were visible, and the six outermost bright spots are from the Ni(111) surface. Note that the threefold symmetries of the substrate and multiple diffraction rings are apparent in (a).